IEEE Access
Multidisciplinary | Rapid Review | Open Access Journal

Received May 7, 2019, accepted May 18, 2019, date of publication May 29, 2019, date of current version June 26, 2019.

Digital Object Identifier 10.1109/ACCESS.2019.2919691

A Valveless Piezoelectric Micropump Based on Projection Micro Litho Stereo Exposure Technology

JUN HUANG[1], LEI ZOU[1], PENG TIAN[1], QUAN ZHANG[2], YUAN WANG[3], AND JIAN-HUI ZHANG[4]

[1]National Research Center of Pumps, Jiangsu University, Zhenjiang 212013, China
[2]School of Mechatronic Engineering and Automation, Shanghai University, Shanghai 200072, China
[3]College of Communication Engineering, Army Engineering University of PLA, Nanjing 210007, China
[4]College of Mechanical and Electrical Engineering, Guangzhou University, Guangzhou 510006, China

Corresponding authors: Quan Zhang (lincolnquan@shu.edu.cn) and Jian-Hui Zhang (zhangjh@nuaa.edu.cn)

This work was supported in part by the National Natural Science Foundation of China under Grant 51605200 and Grant 51605271, in part by the Senior Talent Start-Up Foundation of Jiangsu University under Grant 14JDG145, in part by the Natural Science Foundation of Shanghai under Grant 19ZR1474000, and in part by the Industry-Academia-Research project of Guangzhou University under Grant 2018A001.

ABSTRACT At present, the micropumps are usually adopted in microelectromechanical systems (MEMS) process, which is characterized by high technical complexity and expense, to obtain micro-scale internal channels. Moreover, the MEMS process is more suitable for the 2.5-dimensional channels. This paper presents a 3-dimensional vortex tube-based valveless piezoelectric micropump with low cost and high accuracy, and the projection micro litho stereo exposure (PμLSE) technology is applied to manufacture the prototype of the micropump. The working principle of the piezoelectric micropump is analyzed, and the flow resistance of the vortex diode is calculated numerically. Then, the performance and 3D morphology measurement of the micropump are conducted. The results demonstrate that the inner surface of the channel is uniform and the surface roughness is small. By comparing and analyzing the output performances between two prototypes manufactured by the PμLSE technology, the stability of the PμLSE technology is confirmed. This paper provides a fast and cheap method for manufacturing a 3D micropump, and the proposed approach can also be further adopted in fabricating such micro-stereoscopic structure devices.

INDEX TERMS Piezoelectric pump, valveless, vortex diode, projection micro litho stereo exposure.

I. INTRODUCTION

Piezoelectric actuators have been widely developed and applied in engineering fields with the commercialization of advanced smart materials [1]–[7]. The piezoelectric pump is one of the piezoelectric actuators. The first piezoelectric pump is proposed to transmission insulin in 1978 [8]. As a kind of diaphragm pump, piezoelectric pump has the advantages of no electromagnetic interference, small size, low energy consumption and accurate output, and is widely applied in the fields of drug delivery, fuel cells and heat dissipation systems[9]–[15]. Thus, various types of such pumps have been proposed [16]–[19]. Among all kinds of piezoelectric pumps, valveless piezoelectric pumps, which possess the advantages of simple structure and high reliability, are received much more attentions [20]–[27].

The fluidic diodes are commonly employed in valveless piezoelectric pumps as no-moving-parts valves to realize fluid flow in one-way. However, due to the differences of the prescribed pressure, the export flow rates of the fluidic diode in different flow direction are not equal. Therefore, similar to the electrical diode, the fluidic diode possesses the feature of unidirectional continuity. Once the pressure difference is determined, the efficiency of the fluidic diode is defined as the ratio of the flow difference between the forward and the reverse flows to the forward flow. The Tesla tube [28], diffuser/nozzle [29] and Y-shape tube [30] are three well-known diode types which are commonly used in valvless piezoelectric pumps. Anduze *et al.* [31] proposed a new vortex diode and compared to the classical diode.

The associate editor coordinating the review of this manuscript and approving it for publication was Yingxiang Liu.

The results demonstrated that the efficiency of the vortex diode was equivalent to or even slightly better than Tesla tube and diffuser within a certain range of prescribed pressure difference. Hence, the valveless piezoelectric micropump with vortex diodes using as no-moving-part valve is proposed in this study.

The valveless piezoelectric micropumps are formerly processed on silicon wafers or glass by lithographic technique. For example, Gerlach and Wurmus [32], Gerlach [33] etched the square diffuser/nozzle and pump chamber on silicon wafer by chemical method. The borosilicate glass was applied as the cover anodic bonding with the silicon wafer to fabricate piezoelectric micropump. This processing method was mature and possessed high processing accuracy, but such approach suffered the disadvantages of expensive and time-consuming. Recently, a processing method of replication technology, in which the PDMS (polydimethylsiloxane) based polymer are applied as a base material, has been widely investigated, such as hot-embossing technology and soft lithography technology [34], [35]. Although such kind of processing technology was much simpler and cheaper compared to the lithographic technique, a corresponding mask, which is not suitable for rapid prototyping, was necessarily required. In general, the above methods were only applicable to processing of 2.5-dimensional channel, but hardly for 3D complex geometry with relatively lower cost. With the development of 3D printing technology, this situation has been improved. Zhang *et al.* [36] utilized the fused deposition modeling (FDM) technology to fabricate a valveless piezoelectric pump with triangular prism bluff body. The depth of the pump chamber was 4mm, and the side length of the triangular prism was 5mm. The technology features the advantages of convenient and cheap fabricating procedure, especially for the devices with complex structures. However, it was unsuitable for micropump manufacturing due to the relatively low process precision. The projection micro litho stereo exposure (PμLSE) technology was another 3D micro/nano printing processing method, which can produce 3D micro-channel structures with high accuracy.

In this paper, a novel valveless piezoelectric micropump was designed with a vortex diode as the ''valve''. In order to analyze the forward and reverse flow resistance, the internal flow field of the vortex diode was calculated through finite element method. Then, the prototype of the micropump was manufactured by the PμLSE technology, and the experiments were implemented to obtain the performances and the processing effects of the micropump.

II. STRUCTURAL DESIGN AND WORKING PRINCIPLE

The vortex diode consists of 3 parts: an axial tube, a vortex chamber, and a tangential tube. In this study, the procedure that the fluid flowing through the axial tube, the vortex chamber and the tangential tube in sequence is defined as the forward flow. On the contrary, the back flowing sequence is defined as the reverse flow. Fig.1 is the schematic diagram of the working principle of the vortex diode. In the forward flow,

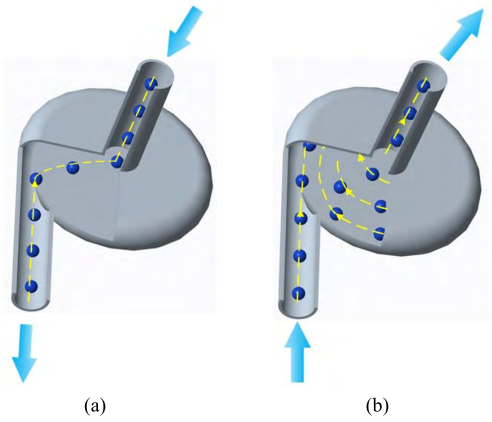

FIGURE 1. The working principle of the flow in vortex diode. (a) The forward flow. (b) The reverse flow.

energy loss occurs only at the position where the axial tube and the tangential tube connecting with the vortex chamber. Alternatively, the flow resistance and energy loss in the forward flow are relatively slight. However, in the reverse flow, the fluid forms a vortex motion in the vortex chamber, which leads to an increasing flow resistance and a large energy loss. Specifically, due to the difference between the flow resistance in forward and reverse flow, the vortex diode acts as a check valve.

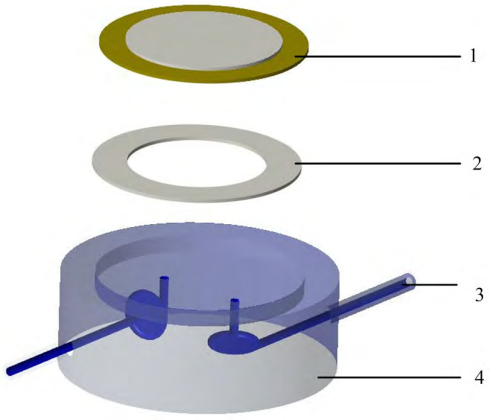

FIGURE 2. Schematic diagram of the valveless piezoelectric pump with vortex diodes: 1. Piezoelectic vibrator; 2. Sealing ring; 3. Vortex diode; 4. Pump body.

Fig. 2 shows an exploded view of the designed valveless piezoelectric micro-pump with vortex diodes in this study. The micropump mainly consists of a piezoelectric vibrator, a sealing ring, and a pump body. The pump body contains a pair of vortex diodes and a pump chamber.

When applying an AC voltage to the piezoelectric vibrator, the shrink and stretch motions of the vibration in the radial direction are produced, leading a volume change of the pump chamber. In stretch motion, the pressure of the inside chamber is getting decreased with the increasing of the pump chamber volume, and hence the external fluid is forced to flow into the

pump chamber through two vortex diodes by the differences of the inside and outside pressure. Such process is referred as the suction procedure. Conversely, the pressure of the inside chamber is getting increased with the decreasing of the pump chamber volume, leading the phenomena that the internal fluid flowing out of the pump chamber through the two vortex diodes, such process is defined as the discharge procedure. Due to the flow resistance inequality of the vortex diodes in the forward and reverse directions, the fluid flow passing through the tangential pipe and axial pipe of the piezoelectric pump is different during the suction and discharge processes. Furthermore, the macroscopic unidirectional transportation of the fluid is realized in a vibration period of the valveless piezoelectric micropump.

The flow resistance coefficient ξ is applied to characterize the resistance in the vortex diode, and is defined as follows:

$$\xi = \frac{2\Delta P}{\rho v^2} \tag{1}$$

$$\mathrm{Re} = \frac{\rho v d}{\mu} \tag{2}$$

$$\xi = \frac{2\rho d^2 \Delta P}{\mathrm{Re}^2 \mu^2} \tag{3}$$

where, ΔP is the pressure difference between the tangential tube and the axial tube of the vortex diode, v is the outflow velocity of the fluid, ρ is the fluid density, and d is the diameter of the channel.

The flow of the valveless piezoelectric micropump can be approximated as [29]:

$$Q = \Delta V f = 2 f V_x \left[\frac{\eta^{1/2} - 1}{\eta^{1/2} + 1}\right] \tag{4}$$

$$\eta = \frac{\xi_R}{\xi_F} \tag{5}$$

$$V_x = \pi D R^2 \tag{6}$$

where, ΔV is the volume change of the pump chamber within a half vibration period, D is the amplitude of the piezoelectric vibrator, R is the radius of the piezoelectric ceramic, f is the driving frequency of the piezoelectric vibrator, ξ_R is the reverse flow resistance coefficient of the vortex diode, and ξ_F is the forward flow resistance coefficient of the vortex diode.

III. THE FINITE ELEMENT ANALYSIS

A 3D model of the fluid domain for the vortex diode is established, with the parameters presented in Table 1. The transition section between the tangential tube and vortex chamber is meshed with unstructured grids. The rest parts

TABLE 1. The parameters of the vortex chamber structure.

Name	Parameters (mm)
Diameter of the axial tube	0.25
Diameter of the tangential tube	0.25
Diameter of the vortex chamber	1.5

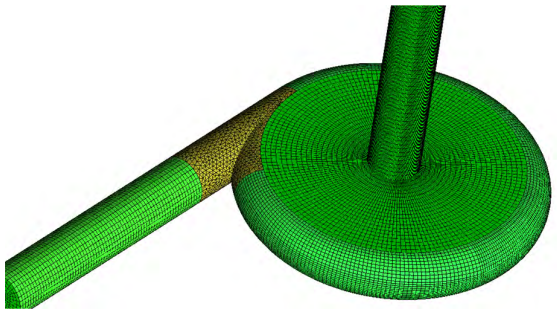

FIGURE 3. The finite element model of the vortex diode.

are meshed with structured grids, and the total number of the elements are 3.8 × 105, as shown in Fig. 3. The forward and reverse flow resistance coefficients of the vortex diode are analyzed by ANSYS CFX. During the forward flow, the fluid flows to the bottom of the vortex chamber first, and then flows uniformly to the circumferential wall. There is no strong vortex motion has been observed, and hence the $k-\varepsilon$ model can be adopted for the forward flow. However, during the reverse flow, there is a complex vortex motion existed, and the RNG $k-\varepsilon$ model is chosen to modify the calculation of the velocity gradient flow field. Based on RNG $k-\varepsilon$ model, the calculated accuracy of the vortex motion is improved, and the calculation time is also reduced [38]. For the surface of the wall, the non-slip boundary condition is prescribed. For the calculation of the forward and reverse flows, the inlet surface is set as the pressure inlet, while the outlet surface is set as the open boundary, with the pressure defined as the standard atmospheric pressure.

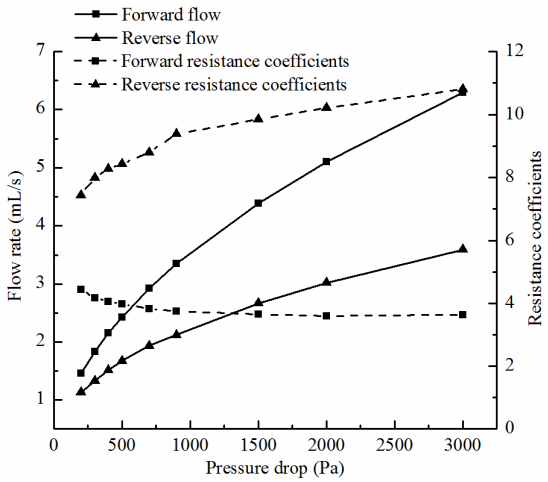

FIGURE 4. The simulation results of the flow rates and resistance coefficients.

The relationship between the pressure difference ΔP and the flow rate Q is obtained through the simulation results from the forward and reverse flows. Substituting the simulation results into equation (1), the flow resistance coefficients of the vortex diode are calculated under different ΔP, as shown in Fig. 4. The results show that the resistance coefficient of

the forward flow is always smaller than the reverse flow, and the differences of the flow resistance coefficient between the forward and reverse are increased gradually as the ΔP raises. The calculation result also reveals that the flow resistance coefficients of the vortex diode are not equal for the forward and reverse flow, which indicates that the vortex diode can be regarded as a valve for a valveless piezoelectric micropump.

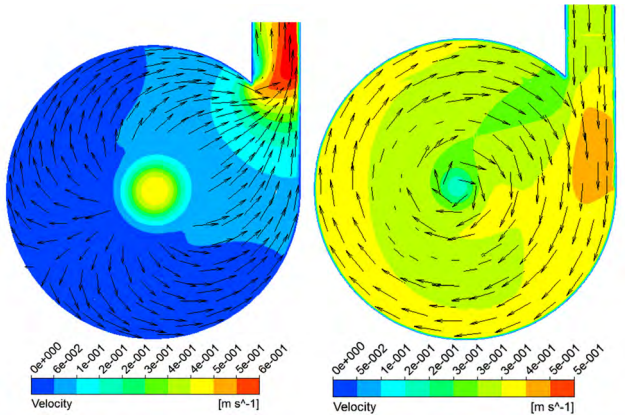

(a) (b)

FIGURE 5. The velocity vector at middle cross section of the vortex chamber (P = 500Pa). (a) The positive flow. (b) The reverse flow.

Fig. 5 shows the velocity vector diagram of the forward and reverse flow at 500Pa. In the forward flow, the streamline of the fluid in the vortex diode is more regular, and there is no vortex phenomena appeared. Compared to the reverse flow, the energy loss is less, and the flow resistance is much smaller. While in the reverse flow, a sharp vortex motion occurs in the vortex chamber and the axial tube, which results in more energy loss and higher flow resistance.

IV. MICROPUMP FABRICATION AND EXPERIMENT

The traditional processing methods are mainly based on the MEMS technology, and silicon is applied as the base material to realize the processing of the pump body through the chemical corrosion, etching, and mechanical bonding procedure. However, such processing approach usually spends a long time and the accuracy is also depended on the experience and proficiency of the operator. The projection micro litho stereo exposure (PμLSE) technology combines the function of both the three dimensional modeling and prototype machining, which only needs to transport the designed 3D model to the processing equipment through computer. Usually the PμLSE method only takes three hours for manufacturing a complicated pump prototype with the size around Φ15mm $\times$ 3.5mm. Moreover, the vortex diode is a stereoscopic structure, and the axial tube, vortex chamber and tangential tube all have a circular cross-section. Hence, the MEMS technology is inappropriate to be applied. The PμLSE technology is employed to manufacture the prototype of the proposed pump, which not only achieves the integrated manufacturing of the internal stereoscopic flow tube, but also improves the accuracy of the inner surface.

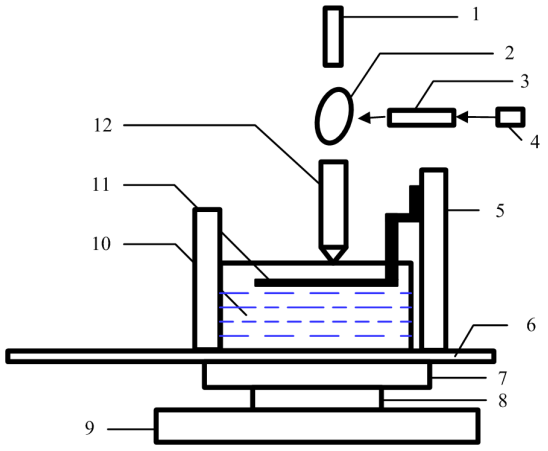

FIGURE 6. Schematic diagram of the 3D micro/nano printing system: 1. Laser displacement sensor; 2. 45° lens; 3.Optical path; 4.Light engine; 5.Z-axis of mobile platform; 6. Mobile platform; 7.X-axis of mobile platform; 8.Y-axis of mobile platform; 9.Marble platform; 10.Resin tank; 11.Prototyping platform; 12.Objective lens.

The PμLSE technology realizes the processing accuracy of 10 μm based on the optical system and the motion platform with high positioning accuracy. Fig.6 is the processing principle diagram. Firstly, the 3D printing slicing software Cura is applied to slice the 3D model required to be processed, and the 2D slices of the model is obtained. Then the ultraviolet rays emitted by the laser are reflected in a digital micromirror device (DMD). The reflected pattern is based on the slicing group produced by Cura, and then the layered resin monomer is exposed by ultraviolet ray. The photosensitive resin in the exposed area rapidly solidifies according to the existed model, and then the high-precision platform moves down to control the depth of the exposure. Hence more photosensitive resin will flow onto the solidified layer, and the fresh resin layer is exposed again by ultraviolet rays. The photosensitive resin at the bottom is not cured since the resin monomer contains a kind of UV absorbing liquid which used to control the depth of the light penetration. Finally, the finished printings can be employed directly as a device, sample, or mold by just cleaning up the residual monomers and curing them.

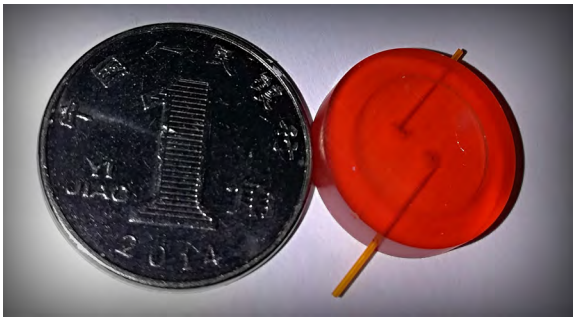

FIGURE 7. Photo of valveless piezoelectric pump with vortex diodes.

A photograph of the micropump is shown in Fig. 7. The size of the piezoelectric micropump is Φ15mm $\times$ 3.5mm,

TABLE 2. Parameters of piezoelectric ceramic.

Parameter	Value
Resonant Frequency Fs	6.0±0.7 kHz
Resonant Impedance Rs	≤600Ω
Free Capacitance(nF)	15±30%
d_{33}	374×10^{-12}C/N

and the diameter D of the circular pump chamber is 10 mm, the depth of the pump chamber is 0.5 mm. The thickness of the seal ring is 0.2 mm, and the inner diameter is 6 mm. The base material of the piezoelectric vibrator is brass, with a diameter of 10 mm and a thickness of 0.2 mm; the piezoelectric ceramic has a diameter of 6 mm and a thickness of 0.2 mm. The parameters of piezoelectric ceramic are shown in Table 2. In order to detect the processing effect of the internal flow channel, the block inside the piezoelectric pump is selected for processing, as shown in Fig.8.

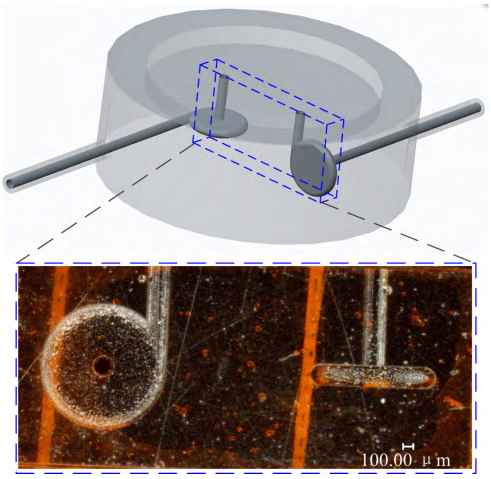

FIGURE 8. The inner block of the piezoelectric pump.

The Keyence's 3D digital microscope with super depth of field (VHX-1000E) is used to measure the inside characteristics of the micropump and observe the processing effect of the inner surface of the channel.

The experimental setup of the piezoelectric micropump is illustrated in Fig. 9. The experimental fluid medium is deionized water. The driving voltage is 200 V and the signal waveform is a sine wave. The output flow rate and output pressure of the micropump are obtained by changing the drive frequency. At the same time, a laser displacement sensor is applied to measure the displacement of the center point of the piezoelectric vibrator working at varied frequencies.

V. RESULTS AND DISCUSSION

Fig. 10 demonstrates the 3D topography scan of the inner surface of the pump chamber at two different locations. The PμLSE technology is cured layer by layer. Under the microscope of ×100 magnification, the cross-sections at A-A, B-B in Fig. 10 are measured, and the results certify

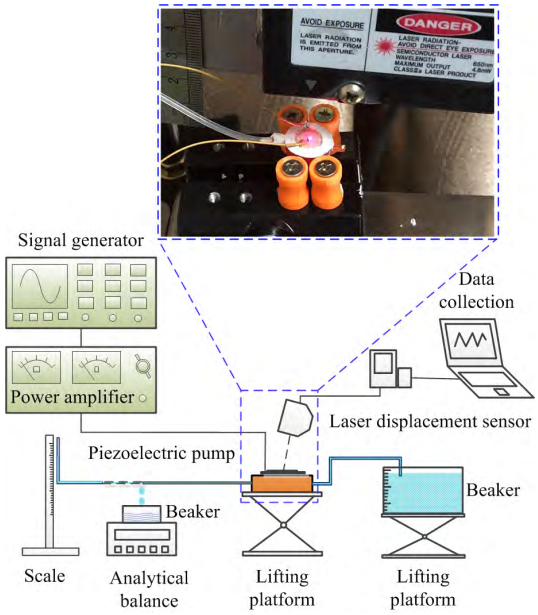

FIGURE 9. Schematic of the experimental setup.

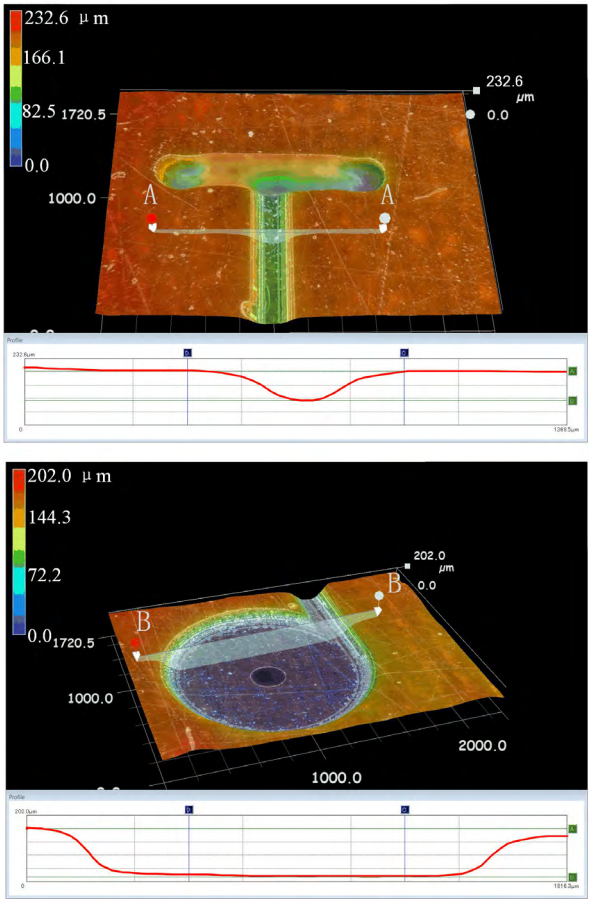

FIGURE 10. The results of 3D topography measurement.

that the inner surface of the vortex diode represent a relatively uniform morphology and smooth shape characteristics. Moreover, the roughness characteristics of the bottom

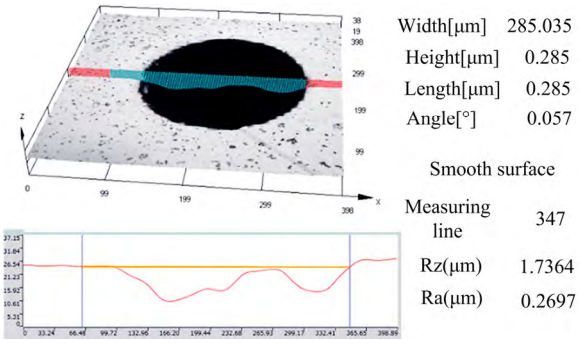

FIGURE 11. The results of the roughness measurement.

surface of vortex diode are measured by the optical digital microscope (OLYMPUS DSX500) in Fig. 11. The test results reveal that the minimum roughness of the bottom of the vortex diode chamber is 0.2697μm. For the channel of the micropump, the frictional resistance is mainly caused by the machined wall. Hence the smaller the roughness of the wall has, the smaller the flow resistance is, resulting in a relatively low energy loss for the fluid. In such situation, the stability of the fluid velocity variation in the vortex diode is improved and the energy loss caused by excessive collision due to uneven velocity variation is also reduced. Therefore, the PμLSE technology conveniently realizes the integrated manufacturing of the 3D vortex diode, and also achieves high accuracy of the inner surface of the channel.

During the experiments, two prototypes manufactured by PμLSE technology are adopted as the comparisons. Fig 12 (a) shows the piezoelectric vibrator amplitudes at the central point of two prototypes tested through laser displacement sensor. Fig 12 (b) exhibits the comparisons of the experimental output performances and the analytical calculation results between two prototypes. When the driving frequency is ranged from 14Hz to 25Hz, the output performance of the piezoelectric pump is stable. At the driving frequency of 20 Hz, the prototype 1 achieves the maximum flow rate about 35.4μL/min, while the prototype 2 achieves the maximum flow rate about 36.8μL/min at the driving frequency of 19 Hz. Comparing the amplitudes of the piezoelectric vibrators in the two prototypes, both of the prototypes reach the maximum amplitude at frequency of 19Hz, with one of 10.3μm and the other of 9.2μm.

For the analytical flow rate, the volume change ΔV of the two prototypes can be calculated separately according to Eq. 5. Due to the small dimensiones of the prototypes, it is hard to measure and calculate the internal fluid velocities and resistances. However, the maximum output back pressure in the experiments of the valveless pump is measured as 70Pa. The velocities in the finite element analysis at 70Pa are substituted into equation 1, and the flow resistances are obtained. The results of the finite element calculation show that the forward velocity is 0.146m/s and the reverse velocity is 0.17m/s at 70Pa in the vortex chamber. Hence the calculation results of equation 1 show that the forward flow

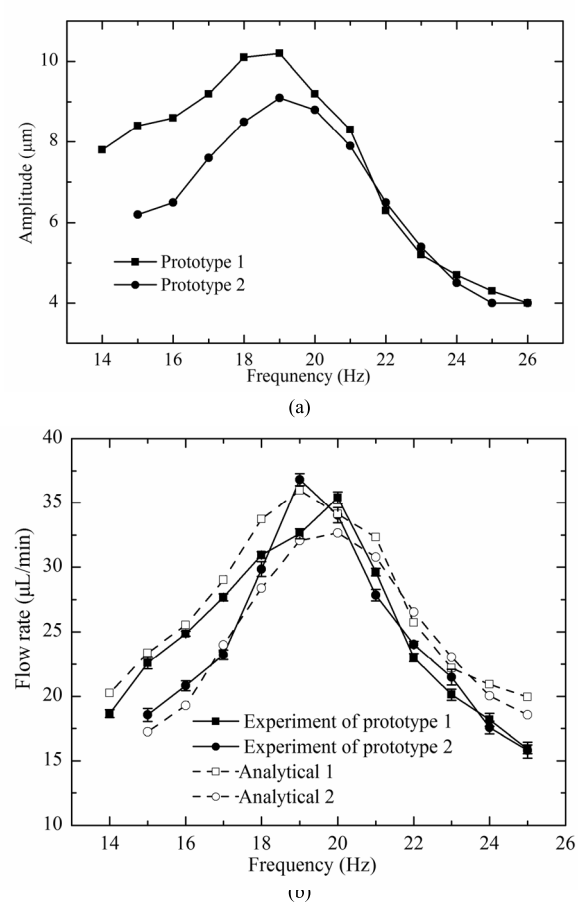

FIGURE 12. The results of piezoelectric pump performance test. (a) Amplitude curve of the piezoelectric vibrator. (b) Curves of the analytical and experimental flow rates.

resistance ξ_F is 4.844 while the reverse flow resistance ξ_R is 6.567. Substituting ξ_R and ξ_F into equation 4, the analytical flow rates of the two prototypes are obtained as shown in Fig. 12 (b). At the driving frequency of 19 Hz, the maximum analytical flow rate of the prototype 1 is 35.96μL/min, while the prototype 2 approaches the maximum analytical flow rate of 32.66μL/min at the driving frequency of 20 Hz.

By comparing and analyzing the output performance of the two prototypes, the stability of the PμLSE technology is confirmed, and the processing error has low influence on the output performance of the pump. Moreover, the PμLSE processing technology provides a new way for the processing of micro piezoelectric pumps.

VI. CONCLUSION

A valveless piezoelectric micropump is designed based on the vortex diode, which possesses the characteristics of flow resistance difference during the forward flow and reverse flow. Considering the fact that the traditional micro fabrication technology is more suitable for the geometric structure of 2.5D, the PμLSE technology is adopted to manufacture the valveless piezoelectric micropump with 3-D sutructure, and the minimum roughness of the pump chamber achieves

0.2697μm. A series of performance tests are carried out based on the valveless piezoelectric micropump with vortex diodes. The results of the experiments demonstrate that the maximum flow rate of the prototype 1 is about 35.4μL/min while the prototype 2 achieves similar value around 36.8μL/min, which confirms the stability of the PμLSE technique.

ACKNOWLEDGMENT

The authors would like to thank the BMF Precision Technology Co, Ltd. for supporting the micro/nano-scale 3D printing work.

REFERENCES

[1] Y. Shi, Y. Li, C. Zhao, and J. Zhang, "A new type butterfly-shaped transducer linear ultrasonic motor," *J. Intell. Mater. Syst. Struct.*, vol. 22, no. 6, pp. 567–575, Apr. 2011.
[2] Y. Shi and C. Zhao, "Simple new ultrasonic piezoelectric actuator for precision linear positioning," *J. Electroceram.*, vol. 28, no. 4, pp. 233–239, Jun. 2012.
[3] Y. Wang and W. Huang, "A piezoelectric motor with two projections using two orthogonal flexural vibration modes," *Sens. Actuators A, Phys.*, vol. 250, pp. 170–176, Oct. 2016.
[4] L. Wang, V. Hofmann, F. Bai, J. Jin, and J. Twiefel, "Modeling of coupled longitudinal and bending vibrations in a sandwich type piezoelectric transducer utilizing the transfer matrix method," *Mech. Syst. Signal Process.*, vol. 108, pp. 216–237, Aug. 2018.
[5] L. Wang, V. Hofmann, F. Bai, J. Jin, Y. Liu, and J. Twiefel, "Systematic electromechanical transfer matrix model of a novel sandwiched type flexural piezoelectric transducer," *Int. J. Mech. Sci.*, vols. 138–139, pp. 229–243, Apr. 2018.
[6] Q. Zhang, C. Li, J. Zhang, and J. Zhang, "Smooth adaptive sliding mode vibration control of a flexible parallel manipulator with multiple smart linkages in modal space," *J. Sound Vib.*, vol. 411, pp. 1–19, Dec. 2017.
[7] Q. Zhang, C. Li, J. Zhang, and X. Zhang, "Synchronized motion control and precision positioning compensation of a 3-DOFs macro–micro parallel manipulator fully actuated by piezoelectric actuators," *Smart Mater. Struct.*, vol. 26, no. 11, Sep. 2017, Art. no. 115001.
[8] W. J. Spencer, W. T. Corbett, L. R. Dominguez, and B. D. Shafer, "An electronically controlled piezoelectric insulin pump and valves," *IEEE Trans. Sonics Ultrason.*, vol. SU-25, no. 3, pp. 153–156, May 1978.
[9] H.-K. Ma, R. H. Chen, N. S. Yu, and Y. H. Hsu, "A miniature circular pump with a piezoelectric bimorph and a disposable chamber for biomedical applications," *Sensors Actuators A, Phys.*, vol. 251, pp. 108–118, Nov. 2016.
[10] X. Y. Wang, Y. T. Ma, G. Y. Yan, D. Huang, and Z. H. Feng, "High flow-rate piezoelectric micropump with two fixed ends polydimethylsiloxane valves and compressible spaces," *Sensors Actuators A, Phys.*, vol. 218, pp. 94–104, Oct. 2014.
[11] H.-K. Ma, S. H. Huang, and Y. Z. Kuo, "A novel ribbed cathode polar plate design in piezoelectric proton exchange membrane fuel cells," *J. Power Sour.*, vol. 185, no. 2, pp. 1154–1161, Dec. 2008.
[12] H.-K. Ma, B.-R. Chen, J.-J. Gao, and C.-Y. Lin, "Development of an OAPCP-micropump liquid cooling system in a laptop," *Int. Commun. Heat Mass Transf.*, vol. 36, no. 3, pp. 225–232, Mar. 2009.
[13] T. Zhan and Q.-M. Wang, "Valveless piezoelectric micropump for fuel delivery in direct methanol fuel cell (DMFC) devices," *J. Power Sour.*, vol. 140, no. 1, pp. 72–80, Jan. 2005.
[14] V. Singhal, S. V. Garimella, and A. Raman, "Microscale pumping technologies for microchannel cooling systems," *Appl. Mech. Rev.*, vol. 57, no. 3, pp. 191–221, Jun. 2004.
[15] B. Ma, S. Liu, Z. Gan, G. Liu, X. Cai, H. Zhang, and Z. Yang, "A PZT insulin pump integrated with a silicon microneedle array for transdermal drug delivery," *Microfluidics Nanofluidics*, vol. 2, no. 5, pp. 417–423, Sep. 2006.
[16] H. J. Sheen, C. J. Hsu, T. H. Wu, H. C. Chu, U. Lie, and C. C. Chang, "Experimental study of flow characteristics and mixing performance in a PZT self-pumping micromixer," *Sensors Actuators A, Phys.*, vol. 139, nos. 1–2, pp. 237–244, Sep. 2007.
[17] X.-F. Leng, J.-H. Zhang, Y. Jiang, J.-Y. Zhang, X.-C. Sun, and X.-G. Lin, "Theory and experimental verification of spiral flow tube-type valveless piezoelectric pump with gyroscopic effect," *Sens. Actuators A, Phys.*, vol. 195, pp. 1–6, Jun. 2013.
[18] K. S. Rao, J. Sateesh, K. Guha, K. L. Baishnab, K. G. Sravani, and P. Ashok, "Design and analysis of MEMS based piezoelectric micro pump integrated with micro needle," in *Microsystem Technologies*, 2018, pp. 1–7.
[19] J. C. Rife, M. I. Bell, J. S. Horwitz, M. N. Kabler, R. C. Y. Auyeung, and W. J. Kim, "Miniature valveless ultrasonic pumps and mixers," *Sensors Actuators A, Phys.*, vol. 86, nos. 1–2, pp. 135–140, Oct. 2000.
[20] S. Singh, N. Kumar, D. George, and A. K. Sen, "Analytical modeling, simulations and experimental studies of a PZT actuated planar valveless PDMS micropump," *Sensors Actuators A, Phys.*, vol. 225, pp. 81–94, Apr. 2015.
[21] Y. T. Ma, F. R. Kong, C. L. Pan, Q. Zhang, and Z. H. Feng, "Miniature tubular centrifugal piezoelectric pump utilizing wobbling motion," *Sensors Actuators A, Phys.*, vol. 157, no. 2, pp. 322–327, Feb. 2010.
[22] F. R. Munas, G. Melroy, C. B. Abeynayake, H. L. Chathuranga, R. Amarasinghe, P. Kumarage, Van T. Dau, and D. V. Dao, "Development of PZT actuated valveless micropump," *Sensors*, vol. 18, no. 5, p. 1302, Apr. 2018.
[23] I. Izzo, D. Accoto, A. Menciassi, L. Schmitt, and P. Dario, "Modeling and experimental validation of a piezoelectric micropump with novel no-moving-part valves," *Sensors Actuators A, Phys.*, vol. 133, no. 1, pp. 128–140, Jan. 2007.
[24] A. Ullmann and Y. Taitel, "The piezoelectric valve-less pump: Series and parallel connections," *J. Fluids Eng.*, vol. 137, no. 2, Feb. 2015, Art. no. 021104.
[25] S. S. Wang, X. Y. Huang, and C. Yang, "Valveless micropump with acoustically featured pumping chamber," *Microfluidics Nanofluidics*, vol. 8, no. 4, pp. 549–555, Apr. 2010.
[26] V. T. Dau, T. X. Dinh, T. Katsuhiko, and S. Susumu, "A cross-junction channel valveless-micropump with PZT actuation," *Microsyst. Technol.*, vol. 15, no. 7, pp. 1039–1044, Jul. 2009.
[27] Q. Xia, J. Zhang, H. Lei, and W. Cheng, "Theoretical analysis and experimental verification on flow field of piezoelectric pump with unsymmetrical slopes element," *Chin. J. Mech. Eng.*, vol. 22, no. 5, pp. 735–744, Jan. 2009.
[28] F. K. Forster, R. L. Bardell, M. A. Afromowitz, N. R. Sharma, and A. Blanchard, "Design, fabrication and testing of fixed-valve micropumps," in *Proc. ASME Fluids Eng. Division*, San Francisco, CA, USA, vol. 234, Nov. 1995, pp. 39–44.
[29] E. Stemme, "A valveless diffuser/nozzle-based fluid pump," *Sens. Actuators A, Phys.*, vol. 39, no. 2, pp. 159–167, Nov. 1993.
[30] J. H. Zhang, Y. L. Li, and Q. X. Xia, "Analysis of the pump volume flow rate and tube property of the piezoelectric valveless pump with Y-shape tubes," *Chin. J. Mech. Eng.*, vol. 43, no. 11, p. 136, 2007.
[31] M. Anduze, S. Colin, R. Caen, H. Camon, V. Conedera, and T. D. Conto, "Analysis and testing of a fluidic vortex microdiode," *J. Micromech. Microeng.*, vol. 11, no. 2, pp. 108–112, Mar. 2001.
[32] T. Gerlach and H. Wurmus, "Working principle and performance of the dynamic micropump," *Sensors Actuators A, Phys.*, vol. 50, nos. 1–2, pp. 135–140, Aug. 1995.
[33] T. Gerlach, "Microdiffusers as dynamic passive valves for micropump applications," *Sensors Actuators A, Phys.*, vol. 69, no. 2, pp. 181–191, Aug. 1998.
[34] A. M.-H. Pun, J. H.-C. Lo, D. C.-H. Louie, and L.-M. Li, *Micro-Fabrication of the Non-Moving Part Valve Micro-Pump by Hot-Embossing Technology* (IFMBE Proceedings), vol. 14, 2007, pp. 242–245.
[35] J.-H. Kim, C. J. Kang, and Y.-S. Kim, "A disposable polydimethylsiloxane-based diffuser micropump actuated by piezoelectric-disc," *Microelectron. Eng.*, vol. 71, no. 2, pp. 119–124, Feb. 2004.
[36] R. H. Zhang, J. H. Zhang, Y. F. Zhu, and P. Y. Li, "3D printed valveless piezoelectric pump with cone bottom surface," *J. Vibrat., Meas. Diagnosis*, vol. 36, no. 2, pp. 378–382, 2016.
[37] J. H. Zhang and S. Y. Wang, "Study of piezoelectric valveless diffuser/nozzle-based fluid pump: One-way flow principle and the pump flow," *Piezoelectrics Acoustooptics*, vol. 23, no. 1, pp. 23–25, 2001.
[38] S.-X. Qu, Y.-H. Wu, Z.-Z. He, and K. Chen, "Surrogate fluid experimental study and CFD simulation on the hydraulic characteristics of vortex diode," *Nucl. Sci. Eng.*, vol. 189, no. 3, pp. 282–289, Mar. 2018.

JUN HUANG received the M.E. degree in nuclear technology and application and the Ph.D. degree in mechanical design and theory from the Nanjing University of Aeronautics and Astronautics, Nanjing, China, in 2009 and 2014, respectively. He is currently an Associate Professor with the Research Center of Fluid Machinery Engineering and Technology, Jiangsu University. He has published about 20 papers and holds 10 patents. His research interests include piezoelectric actuators and sensors. He received the Second Prize from the Science and Technology Progress Awards of Shandong Province, China, in 2016.

LEI ZOU received the B.E. degree in mechanical engineering from the Guilin University of Electronic Technology, Guilin, China, in 2017. He is currently pursuing the M.Sc. degree with Jiangsu University, China. His research interest includes modeling and simulation on piezoelectric micropump.

PENG TIAN received the B.E. degree in power engineering from Jiangsu University, China, in 2016, where he is currently pursuing the M.Sc. degree. His research interest includes design and simulation on the piezoelectric actuators.

QUAN ZHANG received the B.E. degree in mechanical manufacturing and automation and the Ph.D. degree in mechatronics from the Nanjing University of Aeronautics and Astronautics, Jiangsu, China, in 2009 and 2014, respectively. He is currently an Associate Professor with the School of Mechatronic Engineering and Automation, Shanghai University. He has published over 30 papers and holds 10 patents. His research interests include piezoelectric transducers, dynamic modeling, and the vibration control of rigid-flexible manipulators.

YUAN WANG received the B.E. degree from the School of Electrical Engineering, Anhui University of Science and Technology, China, in 2006, and the M.E. degree from the School of Electronic and Optical Engineering, Nanjing University of Science and Technology, China, in 2008. She is currently a Lecturer with the College of Communication Engineering, Army Engineering University of PLA. She has published more than 20 papers. Her research interests include design and control of the piezoelectric actuators, and design on the piezoelectric sensors.

JIAN-HUI ZHANG received the M.E. and Ph.D. degrees in mechanical engineering from National Yamagata University, Japan, in 1998 and 2001, respectively. He is currently a Professor with the College of Mechanical and Electrical Engineering, Guangzhou University. He has published more than 50 papers and holds 50 patents. His research interests include piezoelectric actuator, micro-gyroscope and gears, and chain drive.